

# On Ground Test of An IMU/GNSS Receiver for Atmospheric Re-entry Vehicle Applications

Xiaoliang Wang · Shufan Wu\* · Deren Gong · Zhe Su

Received: 30/May/2019 / Accepted: date

**Abstract** This article introduced the on-ground test of a novel IMU/GNSS integrated navigation system for atmospheric re-entry applications. Dynamic and kinetic model of re-entry vehicle are introduced with proper coordinates, dynamic & kinematic equations for angular motion are also provided by using Eulers Law and quaternions. The principle of SINS mechanization is illustrated, which can be easily inserted into re-entry vehicle GNC closed loop. On-ground and underground vehicle test results are provided which demonstrated the promising performance of this IMU/GNSS receiver for future atmospheric re-entry applications.

**Keywords** IMU/GNSS · HiSGR · SINS · Atmospheric Re-entry · Acquisition & Tracking

## 1 Introduction

The atmospheric re-entry spacecraft like X-38 crew return vehicle (CRV) is a key part for the manned international space station (ISS). It is a spacecraft attached to the ISS, which will serve as a life boat for the astronauts on-board

---

This paper is supported by Shanghai Nature Science Foundation (No. 19ZR1426800), and National Natural Science Foundation of China (No. 91438107).

Shufan Wu\* (Corresponding author)

The School of Aeronautics and Astronautics, Shanghai Jiaotong University Dongchuan road No.800, 200240, Shanghai, China

Tel.: +86-15800537342

Fax: +86-34208597

E-mail: shufan.wu@sjtu.edu.cn; xlwang12321@sjtu.edu.cn

Zhe Su

Institute of Satellite Navigation and Intra-Satellite-Link Technology, Academy of Space Electronic Information Technology East Changan Street No.504, 710100, Xian China

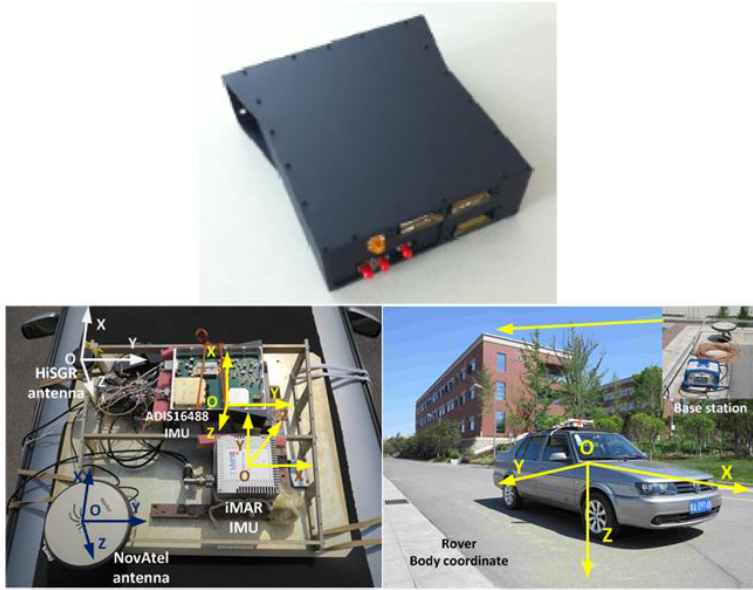


**Fig. 1** HiSGR receiver & on ground test

to come back to Earth, in case of illness and disability of astronauts or other emergencies. It will depart from its docking port, glide from orbit unpowered, re-entry into the Earth atmosphere, and reach a particular landing site by using a steerable parafoil parachute for the final descent to landing[1]-[3].

For atmospheric re-entry vehicle navigation, conventional techniques which used in IMU/GNSS integration for general applications, may not be suitable for this specific case. Because during the blackout phase which covers large part of the re-entry flight, the GPS receiver will have no signal available for the navigation system. So, the IMU will therefore be the only navigation system on-board, and sensor calibration with GNSS data can only be performed during the exo-atmospheric and de-orbiting phases.

Shanghai Jiaotong University and Academy of Space Electronic Information Technology (ASEIT) is currently developing a novel compact spaceborne IMU/GNSS integrated navigation receiver "HiSGR-High Sensitive GNSS Receiver" for future space applications, under the supporting of National Nature Science Foundation, as shown in figure 1. HiSGR is a multi-functional receiver that can be applied in many platforms, depending on the different versions of software burned in, which has been strictly tested both indoor and outdoor[4].

This article concerns the on-ground test of such IMU/GNSS integrated navigation system for atmospheric re-entry applications. Dynamic and kinetic model of re-entry vehicle are introduced with proper coordinates, dynamic & kinematic modelling for angular motion are also provided by using Eulers Law and quaternions. The principle of SINS mechanization is given, that can easily be inserted into re-entry vehicle GNC closed loop. On-ground and un-

derground vehicle test results are provided which demonstrated the promising performance of this IMU/GNSS receiver for atmospheric re-entry applications.

## 2 The Dynamic Modelling and IMU/GNSS Integrated System Design

The dynamic of a re-entry vehicle is of 6 Degree of Freedom-DOF motion, consisting of 3 DOF translational dynamics representing the point-mass trajectory movements, and 3 DOF angular motion dynamics representing the rigid body attitude maneuvers. Both dynamic and kinematic movements should be modelled by equations to get a full dynamic description.

The vehicle can be considered as a mass point in the space. Thus, the Newtons Second Law could be used for the modelling, with reference to the rotating R-frame (see APPENDIX). The position and velocity vectors can be expressed in both Cartesian and spherical coordinates, or their mixtures, resulting in different equations of motion. For convenience of the navigation computation, a mixture of the spherical position variables  $(R, \tau, \delta)$  and the Cartesian velocity variables (ground speed) defined in the vertical frame (see APPENDIX) are used to describe the dynamic equations[5][6].

The dynamic equations for angular motion are obtained from the Eulers Law[7][8]. The kinematic equation is dependent on the method of defining the rotation of the body, which can be performed using quaternions, Euler angles or aerodynamic angles. In this paper, the quaternions are used, which is justified by the absence of singularities in the rotations[7][9]. The equations mentioned above set up a complete 6 DOF dynamic model for the atmospheric re-entry vehicle flight, where 13 state variables are employed. The interested readers could be referred to[1], that are not shown here for concise.

As shown in figure 1, the IMU/GNSS receiver is fixed on the top of moving vehicle. It is basically a Strapdown Inertial Navigation System-SINS. By using the information from gyroscope output, a virtual mathematical platform is established. Then, the attitude transformation matrix is obtained, finally, the measurements from accelerometer can be projected to navigation coordinate. There are some methods for SINS attitude update equation as quaternions, Euler angles or aerodynamic angles. Here we choose quaternions due to the simplicity of computation, which comply with the rotational modelling mentioned above. Considering the output of gyroscope is angle increment, a fixed time increment sampling algorithm is used for quaternion computation.

Moreover, due to the reasons that the position and velocity input information of re-entry vehicle control system are spherical position variables  $(R, \tau, \delta)$  and the Cartesian velocity variables  $(v_\delta, v_\tau, v_r)$ (ground speed), here we choose geographical frame as the navigation coordinate for SINS velocity update, which can be easily rotated from ground speed by  $T_x(\pi) T_z(\pi/2)$ . The principle of SINS mechanization is given in figure 2.

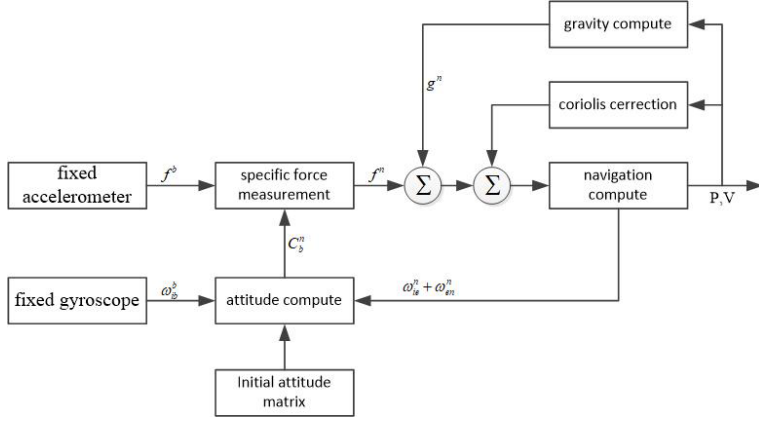


Fig. 2 The principle of SINS mechanization

### 3 SINS error propagation equations

The traditional gyroscope error models are[10]:

$$\begin{aligned}
 \begin{bmatrix} \varepsilon_x \\ \varepsilon_y \\ \varepsilon_z \end{bmatrix} &= \varepsilon = \varepsilon_0 + \varepsilon_w + \delta K_g \omega_{ib}^b + [\delta G \times] \omega_{ib}^b \\
 &= \begin{bmatrix} \varepsilon_{x0} + \varepsilon_{xw} + \delta K_{gx} \omega_{ibx}^b - \delta G_z \omega_{iby}^b + \delta G_y \omega_{ibz}^b \\ \varepsilon_{y0} + \varepsilon_{yw} + \delta K_{gy} \omega_{iby}^b + \delta G_z \omega_{ibx}^b - \delta G_x \omega_{ibz}^b \\ \varepsilon_{z0} + \varepsilon_{zw} + \delta K_{gz} \omega_{ibz}^b - \delta G_y \omega_{ibx}^b + \delta G_x \omega_{iby}^b \end{bmatrix}
 \end{aligned} \tag{1}$$

where  $\varepsilon_0$  denotes gyroscope constant drift,  $\varepsilon_w$  denotes gyroscope random drift,  $\delta K_g$  is scale factor error,  $\delta G$  is installation angle error.

Similarly, the accelerometer error model:

$$\begin{aligned}
 \begin{bmatrix} \nabla_x \\ \nabla_y \\ \nabla_z \end{bmatrix} &= \nabla = \nabla_0 + \nabla_w + \delta K_a f^b + [\delta A \times] f^b \\
 &= \begin{bmatrix} \nabla_{x0} + \nabla_{xw} + \delta K_{ax} f_x^b - \delta A_z f_y^b + \delta A_y f_z^b \\ \nabla_{y0} + \nabla_{yw} + \delta K_{ay} f_y^b + \delta A_z f_x^b - \delta A_x f_z^b \\ \nabla_{z0} + \nabla_{zw} + \delta K_{az} f_z^b - \delta A_y f_x^b + \delta A_x f_y^b \end{bmatrix}
 \end{aligned} \tag{2}$$

where  $\nabla_0$  denotes accelerometer constant drift,  $\nabla_w$  denotes random drift,  $\delta K_a$  is scale factor error,  $\delta A$  is installation angle error.

#### 3.1 Attitude error equations

In inertial navigation systems, suppose the computed attitude matrix is  $\tilde{C}_b^n$ , the real attitude matrix is  $C_b^n$ , the transformation between the two is:

$$\tilde{C}_b^n = B C_b^n \tag{3}$$

where  $B$  is transformation matrix from real  $N$  frame to computed  $N$  frame, i.e., the initial alignment attitude error of inertial systems. Usually, the misalignment angles are small that  $B$  can be represented as:

$$B = [I - \Psi] \quad (4)$$

where  $\Psi$  is the skew symmetric matrix of three axis misalignment angles  $\delta\alpha, \delta\beta, \delta\gamma$ :

$$\Psi = \begin{bmatrix} 0 & -\delta\gamma & \delta\beta \\ \delta\gamma & 0 & \delta\alpha \\ -\delta\beta & \delta\alpha & 0 \end{bmatrix} \quad (5)$$

Then the attitude computation equation is :

$$\Psi = I - \tilde{C}_b^n C_b^{nT} \quad (6)$$

The attitude error propagation equation can be obtained by differential as:

$$\dot{\Psi} = -\dot{\tilde{C}}_b^n C_b^{nT} - \tilde{C}_b^n \dot{C}_b^{nT} \quad (7)$$

With some formula derivations, the error propagation equations in matrix form is:

$$\begin{aligned} \dot{\Psi} = & -[I - \Psi] C_b^n [\tilde{\Omega}_{ib}^b - \Omega_{ib}^b] C_b^{nT} \\ & + \tilde{\Omega}_{in}^n [I - \Psi] C_b^n C_b^{nT} - [I - \Psi] C_b^n C_b^{nT} \Omega_{in}^n \end{aligned} \quad (8)$$

where  $\tilde{\Omega}_{ib}^b$  denotes the measured angular rate matrix of vehicle,  $\tilde{\Omega}_{in}^n$  denotes the computed angular rate matrix in  $N$  frame.

Let  $\delta\Omega_{in}^n = \tilde{\Omega}_{in}^n - \Omega_{in}^n$ ,  $\delta\Omega_{ib}^b = \tilde{\Omega}_{ib}^b - \Omega_{ib}^b$ , omitting some small quantity, the matrix form of attitude error propagation equation is:

$$\dot{\Psi} \approx \Psi \Omega_{in}^n - \Omega_{in}^n \Psi + \delta\Omega_{in}^n - C_b^n \delta\Omega_{ib}^b C_b^{nT} \quad (9)$$

With simplify, equation above can be rewritten as:

$$\dot{\Psi} \approx -\omega_{in}^n \times \Psi + \delta\omega_{in}^n - C_b^n \Omega_{ib}^b \quad (10)$$

where  $\Psi = [\delta\alpha \ \delta\beta \ \delta\gamma]^T$ ,  $\omega_{in}^n \times = \Omega_{in}^n$ ,  $\delta\omega_{in}^n \times = \delta\Omega_{in}^n$ ,  $\delta\omega_{ib}^b \times = \delta\Omega_{ib}^b$ .

### 3.2 Velocity error equations

The idea SINS velocity error equation is:

$$\dot{V} = C_b^n \Gamma^b - [2\omega_{ie}^n + \omega_{en}^n] \times V + g_l \quad (11)$$

where  $g_l$  is the local gravity vector, and

$$g_l = g - \omega_{ie} \times [\omega_{ie} \times r] \quad (12)$$

So, the computed velocity error is

$$\dot{\tilde{V}} = \tilde{C}_b^n \tilde{f}^b - [2\tilde{\omega}_{ie}^n + \tilde{\omega}_{en}^n] \times \tilde{V} + \tilde{g}_l \quad (13)$$

Differential of equation (12) and (13), we get the propagation of velocity error equation:

$$\begin{aligned} \delta\dot{V} = & -\Psi C_b^n f^b + C_b^n \delta f^b - [2\omega_{ie}^n + \omega_{en}^n] \times \delta V \\ & - [2\delta\omega_{ie}^n + \delta\omega_{en}^n] \times \delta g \end{aligned} \quad (14)$$

Omitting the coriolis error and gravity vector error, we get:

$$\delta\dot{V} = [f^n \times] \Psi + C_b^n \delta f^b \quad (15)$$

Conventional nonlinear Extended Kalman filter is adopted for this IMU/GNSS Integrated System. The states variables including the inertial error of position, velocity, the bias of gyroscope and accelerometer. Vast literatures introduced the filter design that not provided here for concise[10].

#### 4 On ground test of IMU/GNSS receiver

The HiSGR receiver can process the received signal measurements to compute the navigation solutions. The core of navigation algorithm is achieved by Real-Time Precise Orbit Determination software (RTPODs), which is from collaboration project with Shanghai Astronomical Observatory, Chinese Academy of Sciences[11]-[13]. RTPODs is a compact and portable software package optimized for real-time processing and is designed for use on embedded DSP systems. It makes use of a nonlinear filter as well as precise dynamic models for orbiting applications. The models used in RTPODs include a full EGM-96 70 by 70 gravity field, the DTM 94 atmospheric drag model [14], a solar radiation pressure model, Earth orientation and polar motion models as well as a relativity model. In addition, RTPODs has the capability to utilize the reduced dynamic technique in which empirical accelerations are estimated in order to account for any dynamics left unmodeled [15]. Finally, the Position, Velocity, and Timing (PVT) point solution will be provided when four or more satellites are being tracked, via a single-shot nonlinear least-squares solver, and also provides onboard orbit determination capabilities under sparse observe conditions. When RTPODs operate in dual frequency mode, more observations are used to compute the ionospheric delay and ionosphere-free pseudoranges for each satellite in view.

The RTPODs mainly operate in GNSS stand-alone navigation mode, and can also be switched to integrated navigation mode that incorporate inertial measurements and on-line processed using ultra-tight coupled GPS/inertial Kalman Filter for predicted orbit position, velocity and attitude, which is used to remove the Doppler effects to allow weak signal tracking in some scenarios.

The availability of the source code allows customization of RTPODs for space applications in difference altitude, and the whole software onboard can

**Table 1** Some RTPODs Versions

RTPODs versions	Applications
RTPODs-LEO	Low earth orbit
RTPODs-R	Reflected signal receiving
RTPODs-HEO	High Eccentric orbit
RTPODs-GEO	Geostationary orbit
RTPODs-LUNAR*	Cislunar/orbiting moon
RTPODs-L2*	Helo Lagrange L2
RTPODs-T	Test for ground vehicle

\*Under development.

be totally reconfigured by using commanding and telemetry interface. So far, several modifications have been made for RTPODs, and table 1 listed some verified software versions for future use.

Some of the RTPODs versions for orbiting applications, as low & high earth orbit, have been demonstrated on previous publications [4]. RTPODs-T is a special version that is used for on ground vehicle test of IMU/GNSS function, which is suitable for atmospheric re-entry navigation. Detail design of RTPODs-T (IMU/GNSS integrated SINS algorithm) has been introduced in above sections, here we provided some open field on ground/under ground test results.

The test is conducted in ASEIT working area from 14:15:00 to 15:15:00 08/Apr/2019. Figure 1 demonstrated the assembling of HiSGR in platform with NovAtels SPAN@ integrated navigation system, which is used for the comparison and evaluation of final solutions, the definition of run car coordination and base station during running test are also provided.

Figure 3 demonstrated the reference trajectory from NovAtels SPAN system, by using WAYPOINT software. The black lines and green dots showed the running route both in open ground and underground. Clearly the SPAN system provided the smooth and precise positioning solution for commercial use. Figure 4&5 illustrated the post processing trajectory from both NovAtel SPAN and HiSGR receiver. The bolded purple lines and green lines in figure 5 demonstrated the SPAN system output, both on open field running and underground test, while the green squares and small black dots shown the same output from HiSGR.

The running trajectory underground is intentional selected as the simulation of re-entry vehicle during blackout period, as in figure 6, and surely the receiver achieved quick signal reacquisition when out of underground garage, and HiSGR perform stable during the running test on open field. Position and velocity error is less than 5m and 0.01m/s during on ground test and achieved less than 15m and 0.02m/s during underground. Attitude angle of vehicle and its rate achieved 0.2deg and 0.05deg/s on-ground, and roughly 0.5deg and 0.1deg/s underground.



Fig. 3 Moving trajectory from NovAtel SPAN system

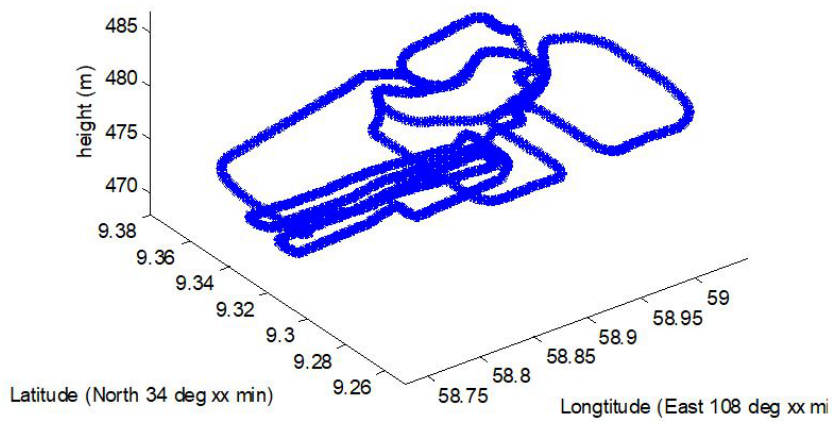


Fig. 4 Processed trajectory from NovAtel SPAN system

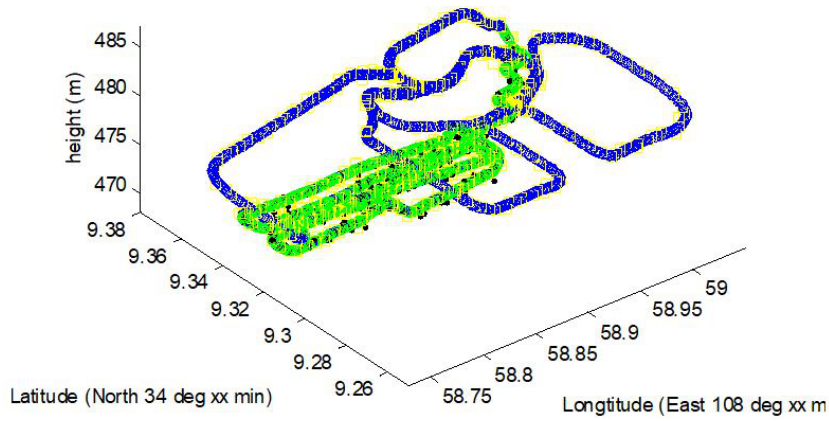
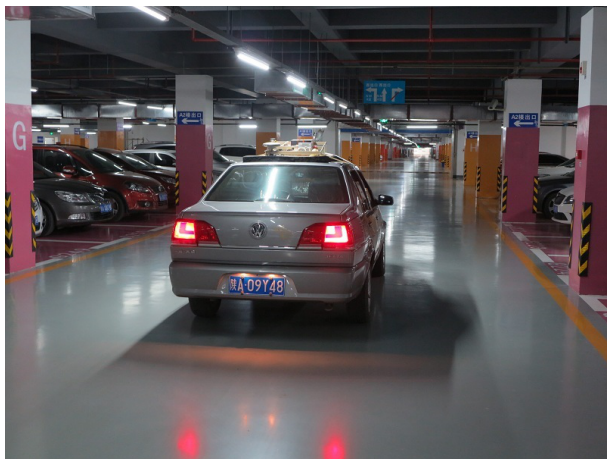


Fig. 5 Trajectory comparison





**Fig. 6** Moving vehicle underground

## 5 Conclusions

This article introduced the on ground test of a novel IMU/GNSS integrated navigation system for atmospheric re-entry applications. Dynamic and kinetic model of re-entry vehicle are introduced with proper coordinates, equations for angular motion are also provided by using Eulers Law and quaternions. The principle of SINS mechanization is given, which can easily be inserted into re-entry vehicle GNC closed loop. On ground and underground vehicle test results are provided that demonstrated the promising performance of this IMU/GNSS receiver for atmospheric re-entry applications.

## 6 APPENDIX

*R-frame* : Earth Centered Earth Fixed frame (index R), the center is in the center of the Earth,  $Z_R$  is pointing North,  $X_R$  is pointing to the Greenwich meridian, and  $Y_R$  completes the right-handed system.

*V-frame* : Vertical Reference frame (index V), the center is in the center of gravity of the body,  $Z_V$  is pointing down collinear with the gravity vector,  $X_V$  is pointing North and  $Y_V$  is pointing East.

*N-frame* : Geographical frame / Navigation frame (index N), the center is in the center of mass of the vehicle,  $Z_V$  is pointing up collinear with the negative gravity vector,  $X_V$  is pointing East and  $Y_V$  is pointing North.

## References

1. Wu S.-F., Costa R.R., Chu Q.-P., Mulder J. A., and Ortega G., "Nonlinear Dynamic Modeling and Simulation of an Atmospheric Re-Entry Spacecraft", *Aerospace Science and Technology*, Vol.5, Issue 5, pp365-381, July 2001
2. NASA Facts, X-38 back to the future for a spacecraft design, <http://www.dfrc.nasa.gov/PAO/PAIS/HTML/FS-038-DFRC.html>
3. NASA Web page, X-38 technology, <http://www.dfrc.nasa.gov/Projects/X38>
4. Xiaoliang Wang, Y Wang Z Su Y Meng D Gong, Design and Test of HiSGR: A Novel GNSS/INS Ultra Tight Coupled Receiver, *Journal of Communications and Information Networks*, 2016 , 1 (3) :67-76
5. Mooij, E. *The Motion of a Vehicle in a Planetary Atmosphere*, Delft University Press, 1997
6. Laban, M., *On-Line Aircraft Aerodynamic Model Identification*, Ph.D. Dissertation, TU Delft, Delft University Press, ISBN 90-6275-987-4, The Netherlands, 1994
7. Regan F.J., Anandakrishnan S.M., *Dynamics of atmospheric re-entry*, AIAA education series, Washington DC, USA, 1993
8. Wu S.-F., Chu Q.-P., *The atmospheric re-entry spacecraft CRV/X-38 C aerodynamic modeling and analysis*, Technical Report, Faculty of Aerospace Engineering, TU Delft, Delft, the Netherlands, Dec. 1999
9. Mooij E., *The motion of a vehicle in a planetary atmosphere*, Report LR-768, Faculty of Aerospace Engineering, Delft, The Netherlands, 1994
10. Fu Mengyin, Zheng Xin, Deng Zhihong, et al. *Transfer alignment theory and application* [M]. Beijing Science Press. 2012:23-34.
11. P.J Li, X.G Hu, Y Huang, G.L Wang, D.R Jiang, *Orbit determination for Chang'E-2 lunar probe and evaluation of lunar gravity models*, *Science China Physics Mechanics & Astronomy*, 2012, 55(3):514-522
12. M Fan, X.G Hu, G Dong, Y Huang, J Cao, *Orbit improvement for ChangE-5T lunar returning probe with GNSS technique*, *Advances in Space Research*, 2015, 56(11):2473-2482
13. Y Huang, M Fan, X Hu, P Li, *The application of GNSS in the near-Earth navigation of Chinas lunar probe CE-5T1*, *Iau General Assembly*, 2015, 21
14. Berger, C., R. Biancale, M. Ill, F. Barlier, *Improvement of the empirical thermospheric model DTM: DTM94 C a comparative review of various temporal variations and prospects in space geodesy applications*, *Journal of Geodesy*, Vol. 72, Issue 3, pp. 161-178, 1998.
15. Wu, S.-C., T. P. Yunck, and C. L. Thornton (1991). *Reduced-dynamic technique for precise orbit determination of Low Earth Satellites*, *Journal of Guidance, Control, and Dynamics*, Vol. 14, No. 1, pp. 24-30.